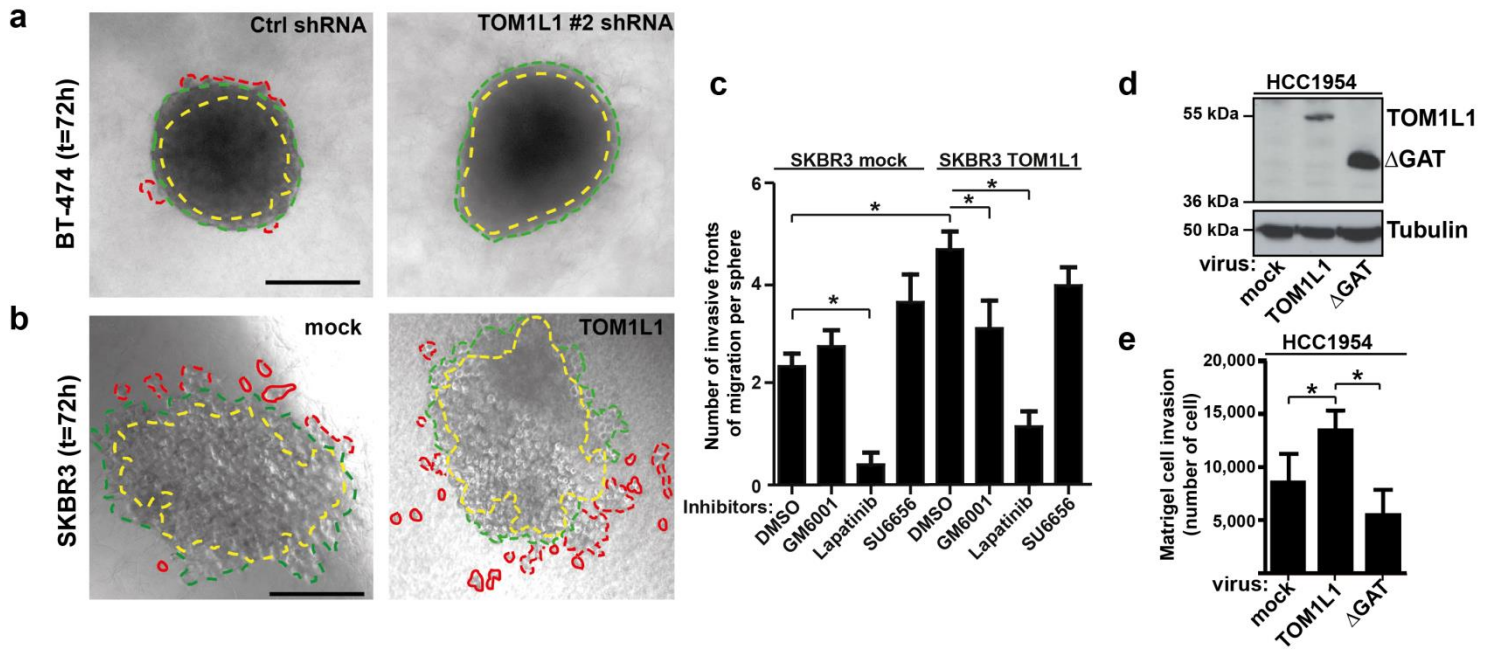
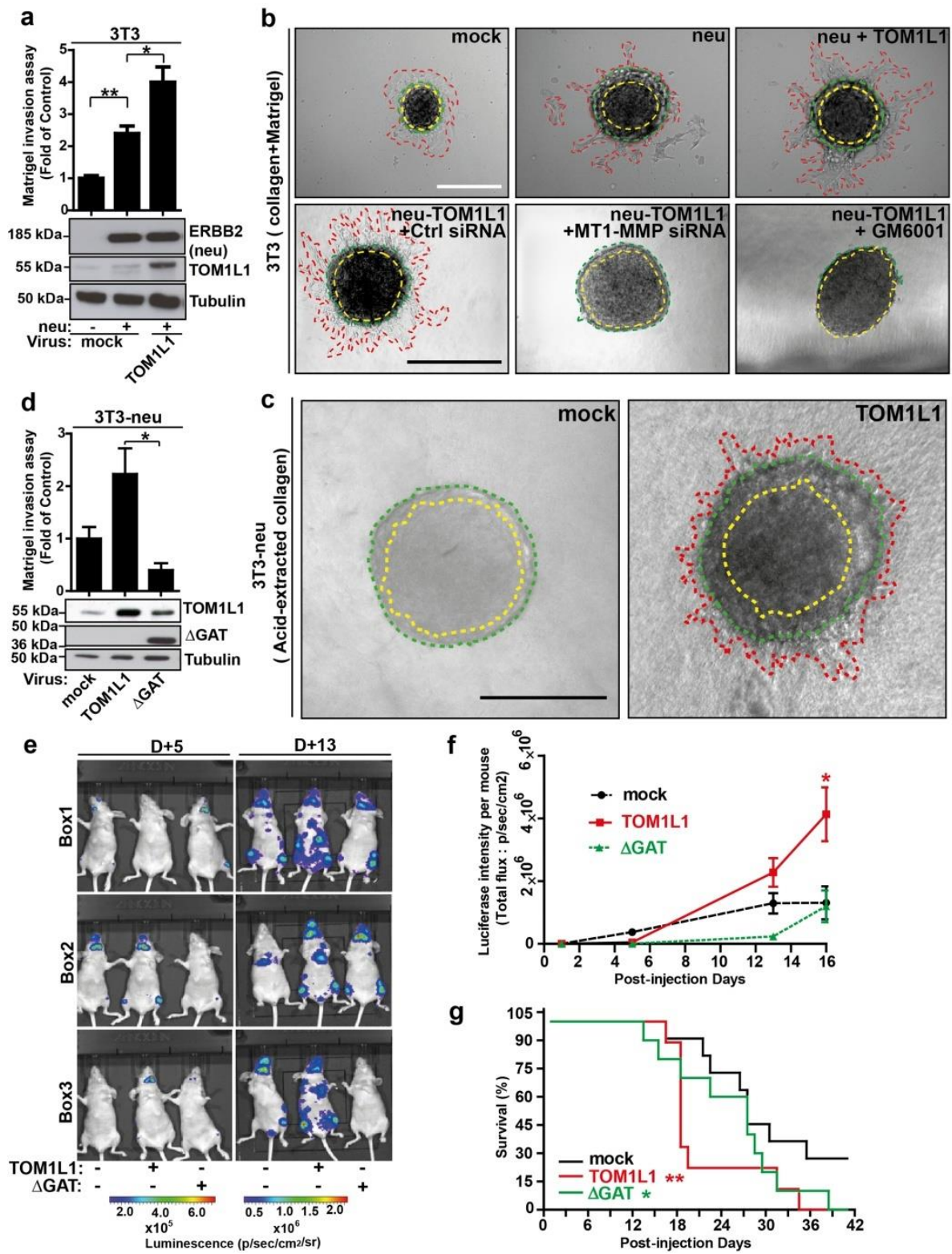


Supplementary Figure 1: TOM1L1 does not regulate cell proliferation nor migration.

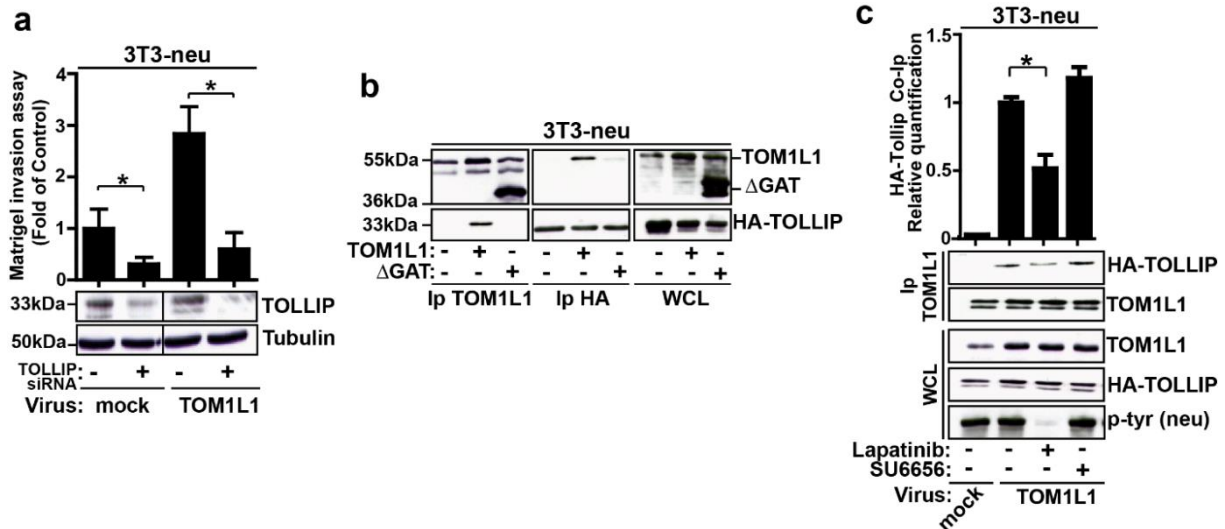
(a) Standard proliferation curves of SKBR3 and BT-474 cells infected with the indicated viruses. (b) Boyden chamber migration assay. 20000 SKBR3, BT-474 or 3T3-neu cells infected with the indicated viruses were seeded in the upper chamber. After 45 min, cells present in the lower chamber were counted in whole well. Histograms (mean \pm SEM) show the cell migration normalized to the control condition (n=3). NS = no-significant (Student's t-test).



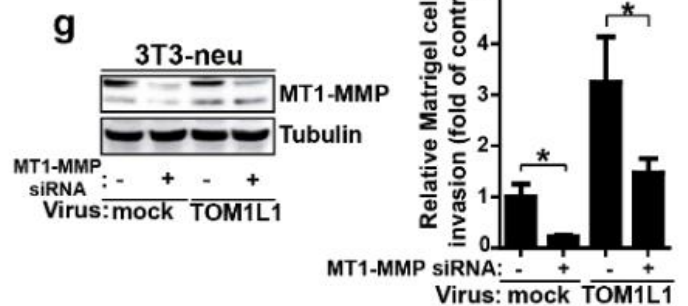
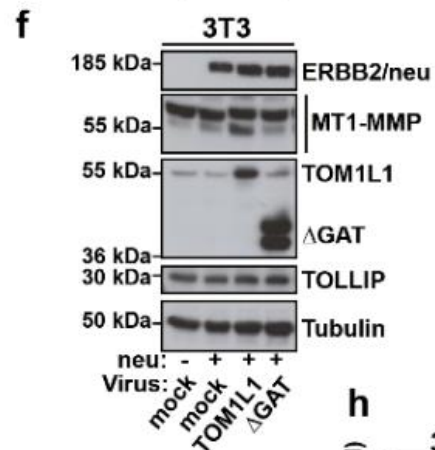
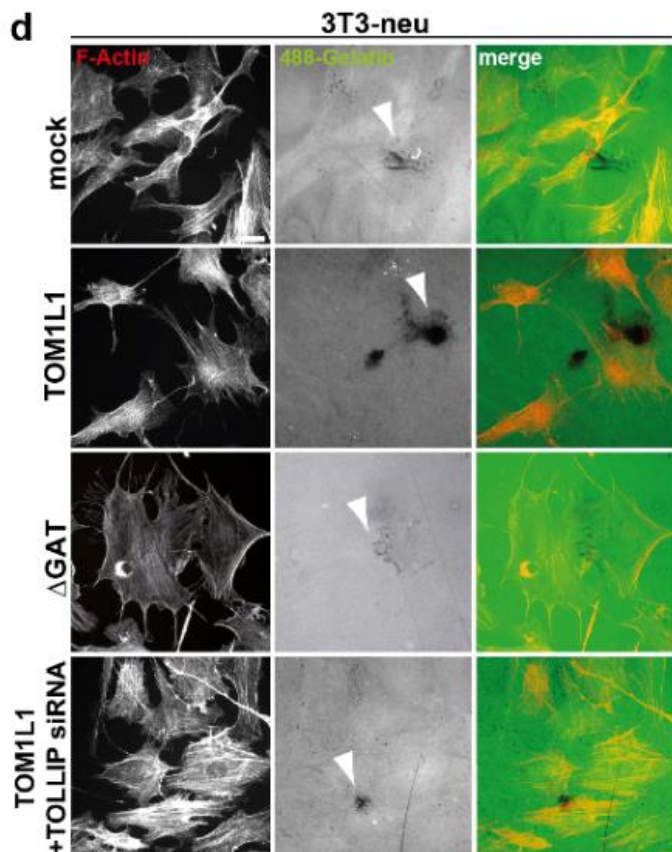
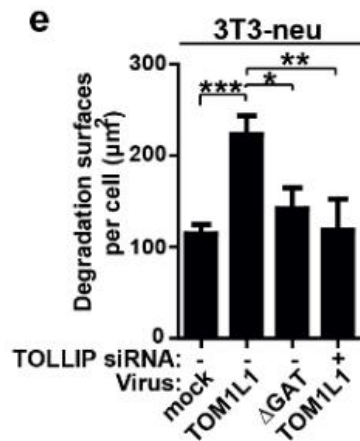
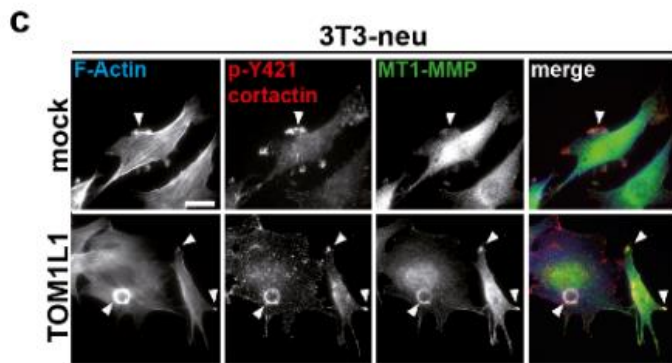
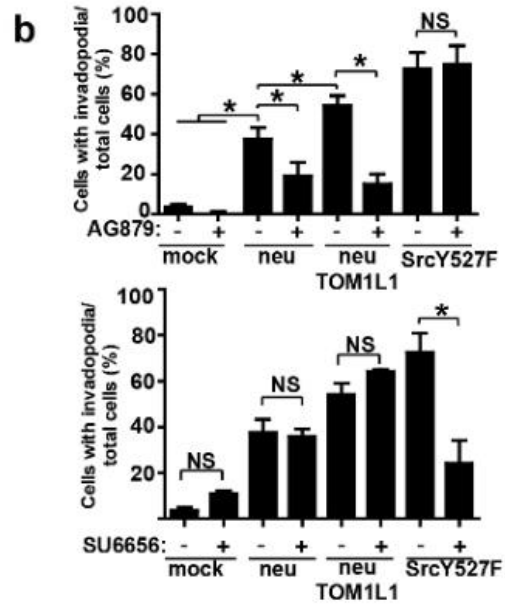
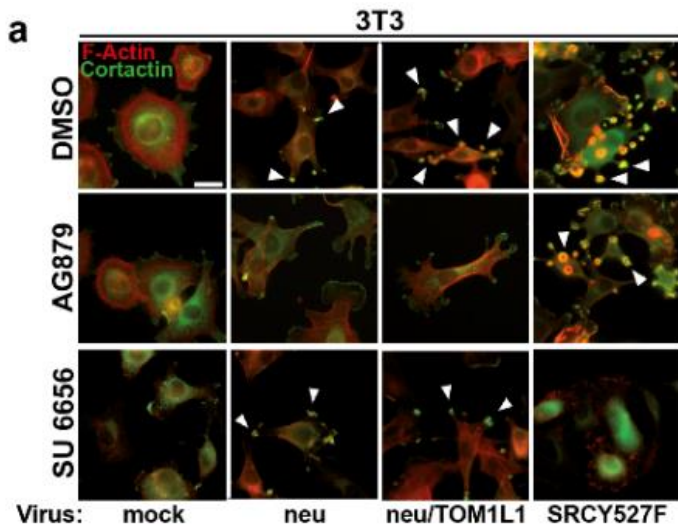
Supplementary Figure 2: TOM1L1 regulates 3D spheroids invasion in rat tail collagen and HCC1954 invasion via its GAT domain. (a-b) Phase contrast images of multicellular spheroids from BT474 (a) and SKBR3 (b) cells infected with the indicated virus or shRNA and embedded in telopeptides intact rat tail collagen I for 72h. Scale bar: 100 μ m. Yellow dotted lines represent size of spheroids at t= 0h. Green dotted lines represent sphere size at the end of the experiment and red dotted line show invasive fronts or cells. (c) Multicellular spheroids from SKBR3 infected as indicated were embedded in a matrix made of a mixture of bovine collagen1 and Matrigel as described in Fig. 2 and incubated for 72h in the presence of DMSO, 12.5 μ m GM6001, 1 μ M Lapatinib, 2 μ M SU6656. Invasive fronts emanating from spheroids were counted (n=4). Shown is the mean \pm SEM *p<0.05 (Student's t-test). (d) HCC1954 cells were infected with the indicated virus and immunoblotted for TOM1L1 or Δ GAT expression. (e) Invasion of HCC1954 cells was assessed onto Boyden chambers coated with Matrigel for 48h and the number of cells in the lower chamber was counted. Shown is the mean \pm SEM (n=3). *p<0.05 (Student's t-test).



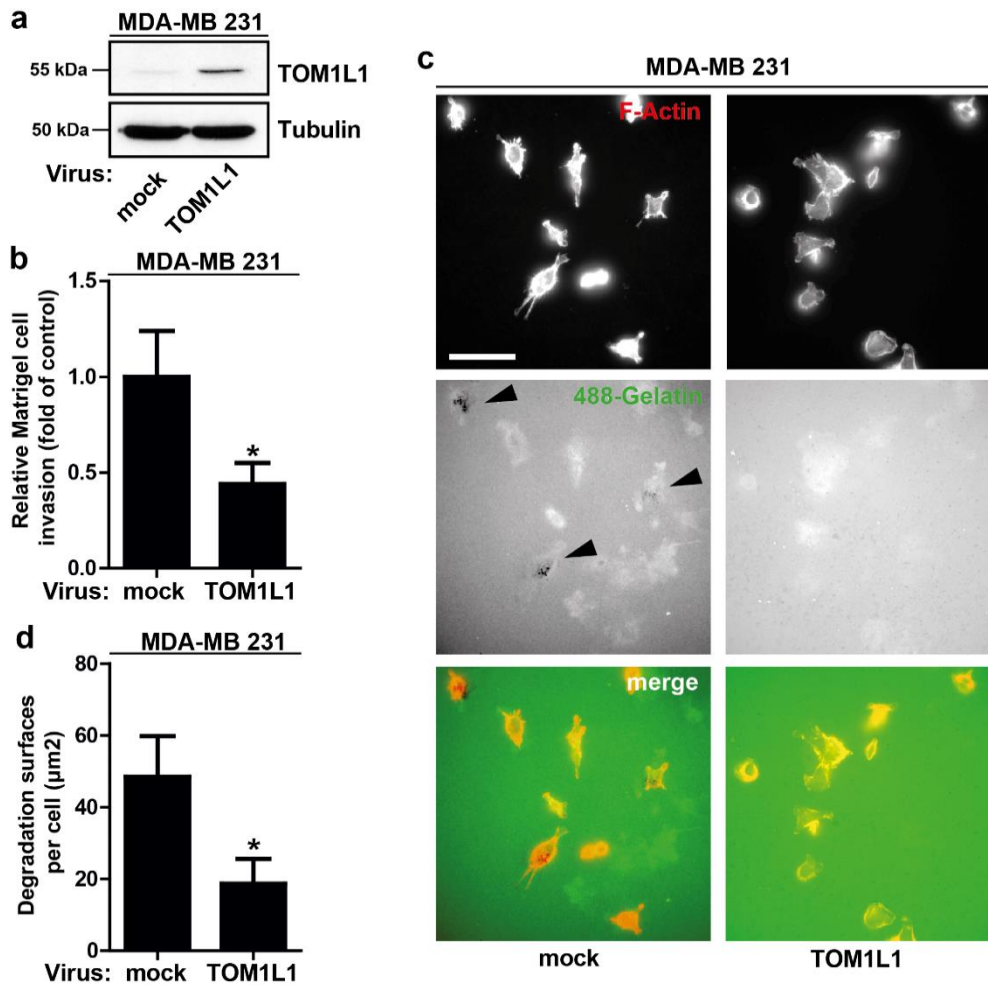
Supplementary Figure 3: TOM1L1 regulates 3T3-neu cell invasion via GAT domain in vitro and in vivo. (a) Lower panel: whole cell lysate of 3T3-neu cells infected and immunoblotted as indicated. Upper panel: invasion of 3T3-neu cells infected with the indicated viruses was assessed in Boyden chamber with Matrigel. Mean \pm SEM *: $p \leq 0.05$ (Student's t-test). (b) 3D spheroid invasion assay. 3T3 cells expressing neu and/or TOM1L1 and transfected with indicated siRNAs or treated with 12.5 μ M of GM6001 for 3h were plated in a 3D collagen/Matrigel matrix. Invasion was observed by timelapse microscopy for 30 to 48 h. (c) Same as in (b) but in telopeptides intact rat tail collagen I and after 72h incubation. Yellow dotted lines represent size of spheroids at $t=0$ h. Green dotted lines represent their size at the end of the experiment and red dotted line show invasive strands. Invasive strands are present in both matrix conditions. Scale bars: 150 μ m. (d) Role of the GAT domain. Top panel: 3T3-neu cells were infected with indicated viruses and were seeded on Boyden chambers coated with Matrigel. Cell invasion was measured as in (a). Bottom panel: western blot showing expression of TOM1L1 and Δ GAT mutant in indicated cells. (e) In vivo invasion assay. One million luciferase-expressing 3T3-neu cells infected with the indicated viruses were injected in the heart left ventricle. 48h later, metastasis formation was imaged in whole body after luciferin injection. Representative images of 3 mice per condition at day 5 and 13 (D+5, D+13) after injection are shown. The color code is indicated in the scale under the images. (f) Quantification of luciferase intensity in time per mouse (mock: $n = 5$, TOM1L1: $n = 5$, Δ GAT: $n = 5$). *: $p \leq 0.05$ (Student's t-test). (g) Kaplan-Meier survival analysis of mice after injection of 3T3-neu cells (mock: $n = 11$, TOM1L1: $n = 9$, Δ GAT: $n = 10$). *: $p \leq 0.05$ (Log-rank, Mantel-Cox test).



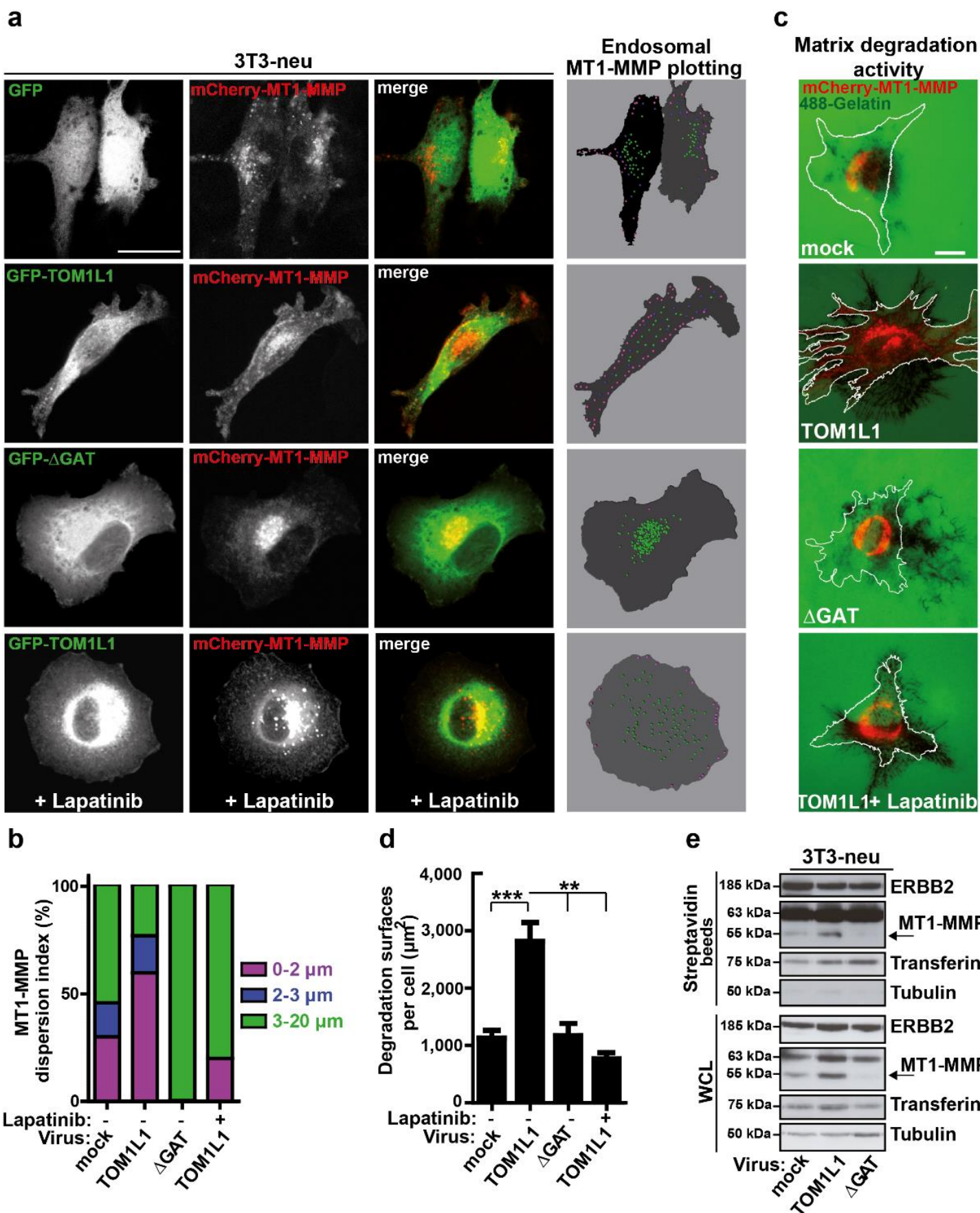
Supplementary Figure 4: TOM1L1 regulates 3T3-neu cell invasion via GAT association with Tollip. (a) Lower panel: 3T3-neu cells infected as indicated were immunoblotted after transfection of anti-mouse Tollip or control siRNAs. Upper panel: 3T3-neu cells infected and transfected as in lower panel were assessed for invasion in Boyden chambers with Matrigel. *: $p \leq 0.05$ (Student's t-test). (b) 3T3-neu cells infected as indicated were transfected with HA-tagged TOLLIP. 48 h after transfection, whole cell-lysates (WCL) were immunoprecipitated (Ip) and immunoblotted as indicated. (c) 3T3-neu cells infected as indicated were transfected with HA-TOLLIP. 48 h after transfection cells were treated with 1 μM Lapatinib or 5 μM SU6656 for 3 h. Lysates were immunoprecipitated and immunoblotted as indicated. Upper graph represents the relative quantification of HA-TOLLIP/TOM1L1 co-immunoprecipitation in 3 independent experiments ($n=3$). Mean \pm SEM. *: $p \leq 0.05$ (Student's t-test).



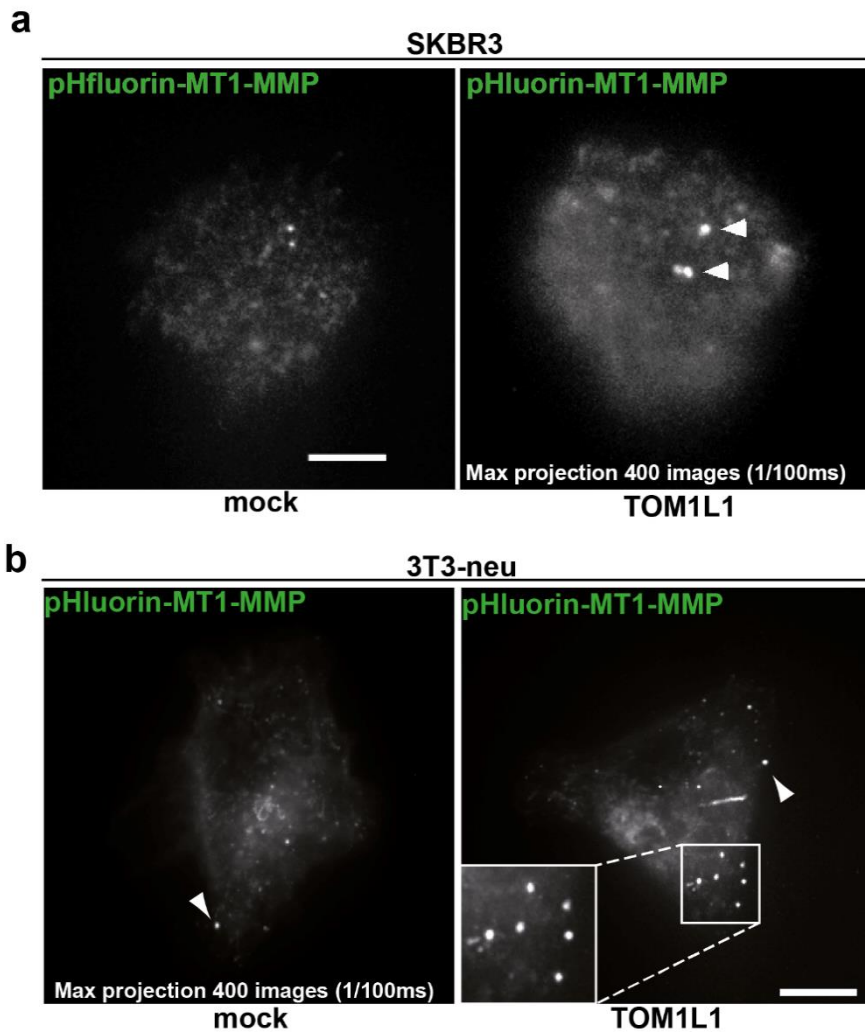
Supplementary Figure 5: The ERBB2-induced TOM1L1-TOLLIP complex regulates invadopodia formation and MT1-MMP activity in 3T3-neu cells. (a) Representative wide-field images showing invadopodia (arrowheads). 3T3 cells infected with the indicated viruses were seeded on Matrigel-coated coverslips with or without 1 μ M AG879 for 3 hours. Cells were stained with Alexa-592 phalloidin for F-Actin detection and immunolabeled for Cortactin. Scale bar: 20 μ m. (b) Quantification of (a): cells with invadopodia were counted and the results normalized to the total number of cells/field (%; n=30-50 cells). *: $p \leq 0.05$; NS: non-significant (Student's t-test). (c) Representative confocal images of F-Actin, p-Y421 Cortactin and MT1-MMP in 3T3-neu cells infected with the indicated viruses. Cells were seeded on gelatin-coated coverslips for 6h at 37°C and immunolabeled using specific antibodies. Arrowheads show colocalization spots. Scale bar: 20 μ m. (d) In situ zymography assays. 3T3-neu cells infected with the indicated viruses and transfected or not with TOLLIP siRNA were seeded on Oregon-Green-488 gelatin-coated coverslips overnight at 37°C to visualize proteolytic activity of the cells (arrowheads). Cells were stained with Alexa-594 phalloidin for F-Actin detection. Scale bar: 20 μ m. (e) Quantification of (d). Histograms represent mean \pm SEM of the degradation surface observed per cell. Mock: n= 87, TOM1L1: n=61, Δ GAT: n=62, TOM1L1 with TOLLIP siRNA: n=22. *: $p \leq 0.05$; **: $p \leq 0.01$; ***: $p \leq 0.001$ (Student's t-test). (f) Western blotting of ERBB2, MT1-MMP, TOM1L1, GAT deletion mutant (Δ GAT) and TOLLIP expression in 3T3-neu cells. Note the apparition of active (55 kDa) isoform of MT1-MMP when TOM1L1 is expressed. (g) 48h after control or MT1-MMP siRNA transfection, whole cell lysates of 3T3-neu cells infected as indicated were immunoblotted for detection of MT1-MMP. (h) 48h after control or MT1-MMP siRNA transfection, invasion of 3T3-neu cells infected with the indicated viruses was evaluated in Boyden chambers with Matrigel.



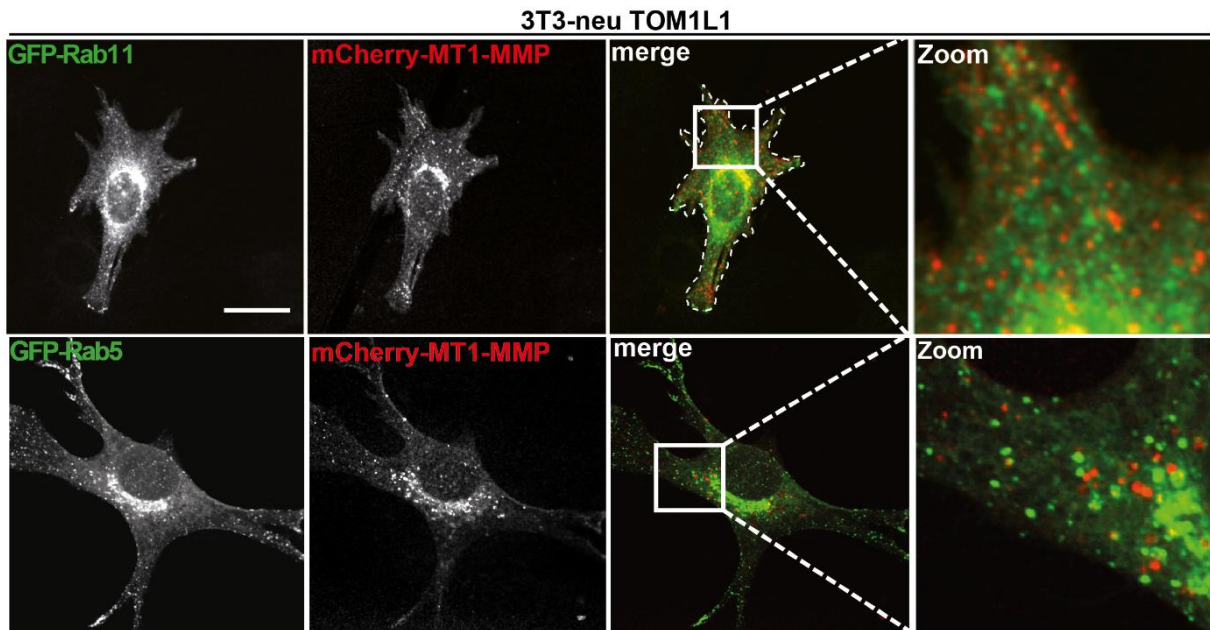
Supplementary Figure 6: TOM1L1 inhibits invasive properties and invadopodia activity of MDA-MB 231 cells. (a) Western blot showing TOM1L1 expression in MDA-MB231 cells infected with the indicated viruses. (b) MDA-MB 231 cells infected with the indicated viruses were assessed for invasion in Boyden chamber with Matrigel. Histograms (mean \pm SEM) show the cell migration normalized to the control condition. (n=3) *: $p \leq 0.05$ (Student's t-test). (c) MDA-MB 231 cells infected with the indicated viruses were seeded on Oregon-Green 488-Gelatin coated coverslips and incubated 3h at 37°C to visualize proteolytic activity of the cells (arrowheads). Cells were stained with Alexa-594 phalloidin for F-Actin detection. Scale bar: 20 μm . (d) Quantification of the matrix degradation area per cell (n=20). Mean \pm SEM *: $p \leq 0.05$ (Student's t-test).



Supplementary Figure 7: TOM1L1 promotes membrane partitioning of MT1-MMP for invadopodia activity and ECM degradation. (a) Left Panel: Representative confocal images showing localization of mCherry-MT1-MMP, GFP-TOM1L1 and GFP-ΔGAT mutant. 3T3-neu cells were transfected with mCherry-MT1-MMP and GFP, GFP-TOM1L1 or GFP-ΔGAT and then plated on gelatin-coated coverslips for 3h treated or not with 1μM Lapatinib. Scale bar, 20 μm. Right panel: Endosomal MT1-MMP plotting. Images were analyzed using the Imaris software and the distribution of the endosomes as a function of their distance from the cell border was quantified. Endosomes located near the border contact are in purple (0-2μm), more cytosolic endosomes (2-3μm) are in blue and endosomes far from the border are in green. (b) Quantification of MT1-MMP dispersion. (c) 48h after mCherry-MT1-MMP transfection, 3T3-neu cells infected with the indicated viruses were seeded on Oregon-Green-488 gelatin-coated coverslips and treated or not with 1μM Lapatinib for 3h to visualize gelatin degradation areas. Scale bar: 10 μm. (d) Histograms show mean ± SEM of the quantification of 25-42 gelatin degradation areas/condition. **: $p \leq 0.01$; ***: $p \leq 0.001$ (Student's t-test). (e) Immunoblotting of cell surface biotinylated ERBB2, MT1-MMP and Transferin receptor after Streptavidin beads precipitation in 3T3-neu cells. Arrows show catalytically active cleaved form of MT1-MMP.



Supplementary Figure 8: MT1-MMP exocytosis. 48h after transfection with MT1-MMP-pHluorin construct as in ref [34], SKBR3 (**a**) or 3T3-neu cells (**b**) were plated on plasma clean glass coverslip coated with gelatin and imaged by TIRF in live (see Supplementary Movies 2 & 3). The max projection of 400 images taken every 100ms during 40s is shown. Arrowheads point exocytose flashes. Insets are higher magnification of the boxed areas showing region of high MT1-MMP exocytosis. Scale bar: 10 μ m.



Supplementary Figure 9: MT1-MMP is not located in RAB5/RAB11-endosomes. 48h after GFP-Rab11 or GFP-Rab5 and mCherry-MT1-MMP transfection, 3T3-neu TOM1L1-expressing cells were plated on gelatin-coated coverslips for 3h to visualize colocalization by confocal imaging. Insets show higher magnification of the boxed areas. Scale bar: 20 μ m.

Fig. 1d

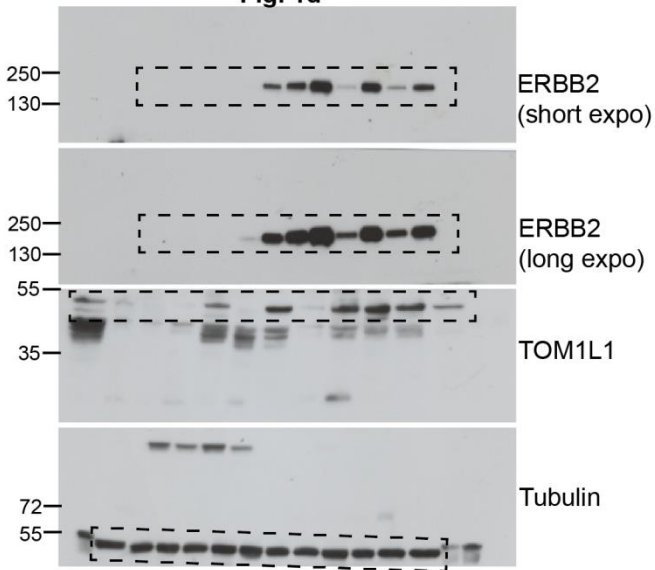


Fig. 2a

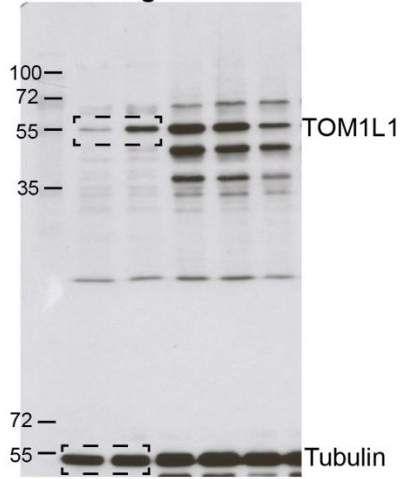


Fig. 2e

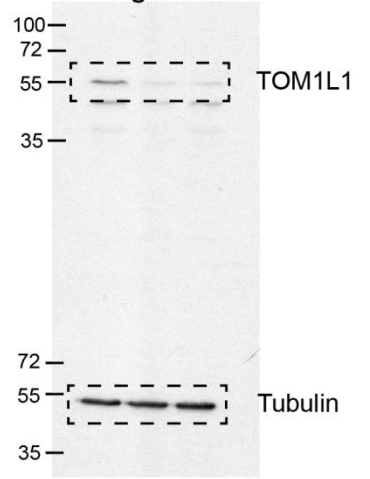


Fig. 3b

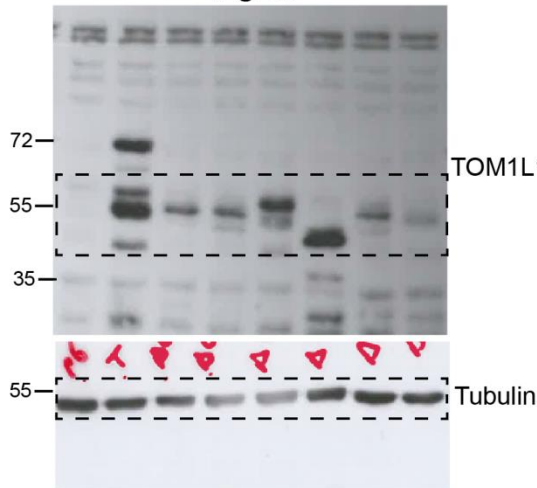


Fig. 3c

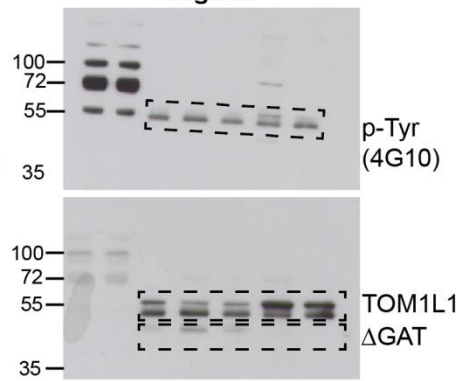


Fig. 3f

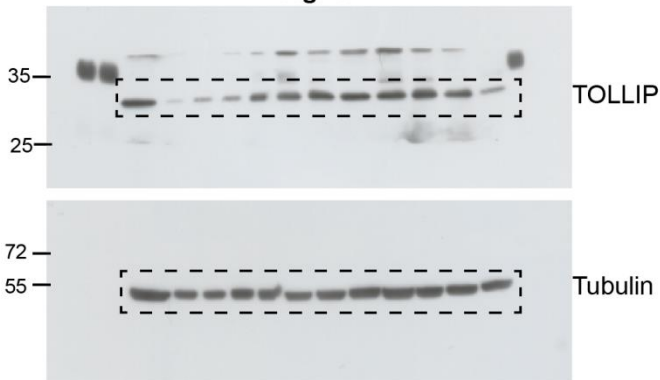


Fig. 3g

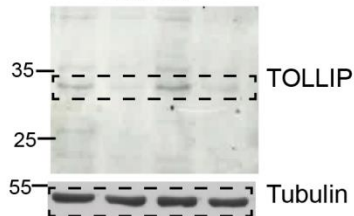
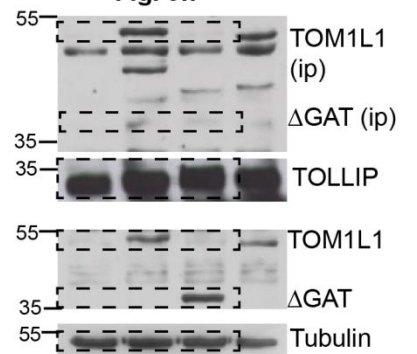
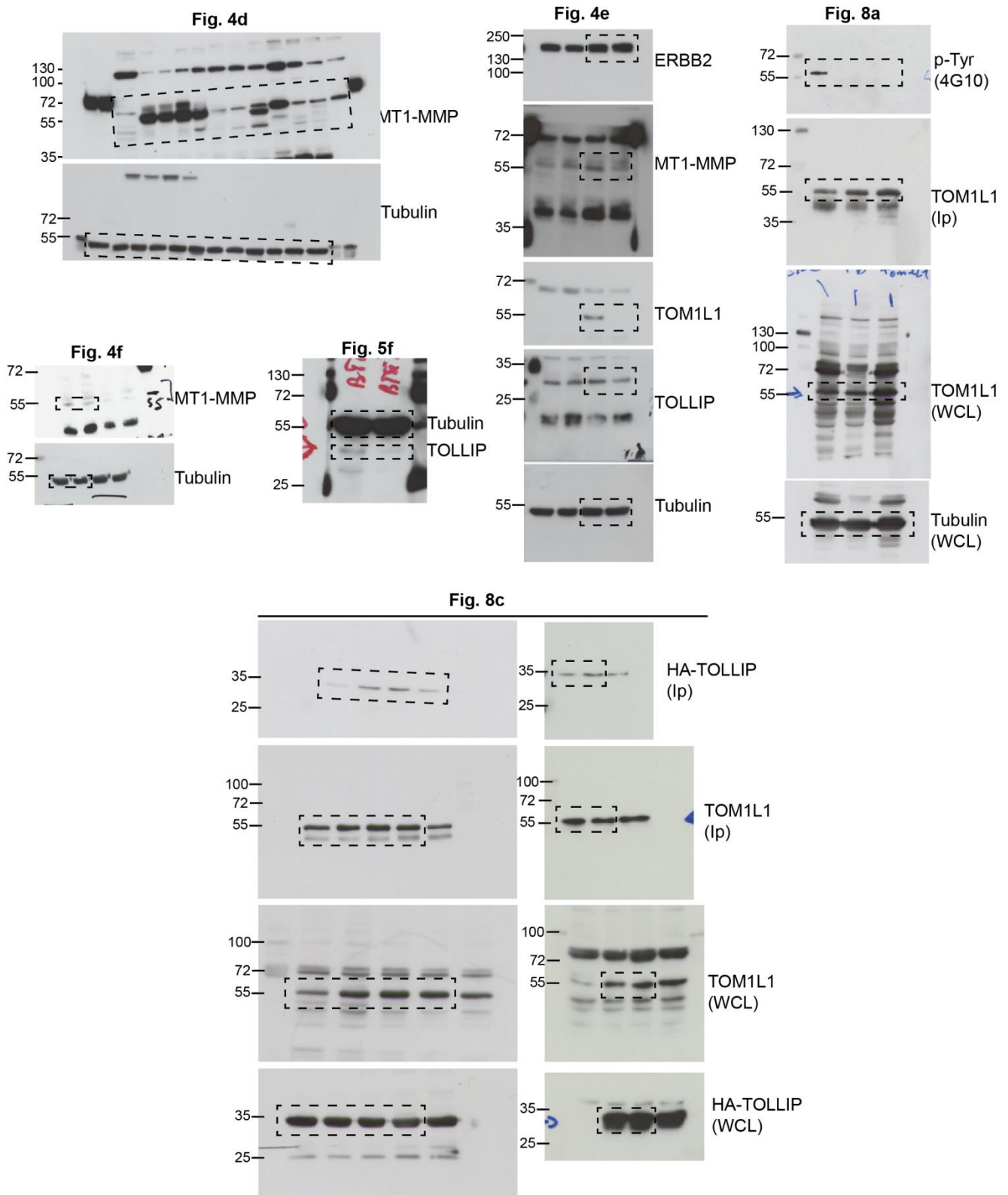


Fig. 3h





Supplementary Figure 10: Western blot images of the selected portion displayed in the main figures. Boxed areas were cropped for designated figures.

Gene Symbol	Cytoband	Gene amplification (%)	Frequency of co-amplification with ERBB2	Bilateral t-test (p values)
ERBB2	17q12	18%	NA	0.0105
TOM1L1	17q22	11%	52.5%	0.0351
CLTC	17q23.1	13%	47.5%	0.0420
RPS6KB1	17q23.2	12%	47.5%	0.0161
PPM1D	17q23.2	15%	45.4%	0.0050

Supplementary Table 1 (related to Fig. 1) Amplification of *ERBB2* and the most frequently co-amplified genes were profiled in a set of 402 breast tumours by array-CGH. The table shows the four most frequently co-amplified genes, their chromosomal localization and frequency of co-amplification.

A	Whole Tumour Set (N = 402)		ER- (N = 142)		ER+ (N = 260)	
	N	%	N	%	N	%
<i>ERBB2</i>	61	15%	32	23%	29	11%
<i>TOM1L1</i>	42	10%	17	12%	31	12%
<i>ERBB2/TOM1L1</i> <i>Co-amplification</i>	32	8%	13	9%	19	7%
B	ERBB2 amplified Tumours (N = 61)		ER- (N = 32)		ER+ (N = 29)	
	N	%	N	%	N	%
<i>TOM1L1</i>	32	52%	13	41%	19	66%
						p = 0.025

Supplementary Table 2 (related to Fig. 1) A: Frequency of *ERBB2* and *TOM1L1* amplification and co-amplification in a set of 402 breast tumours analysed by RT-qPCR. Frequencies are presented for the complete set of tumours and for the Oestrogen Receptor-negative (ER-) and -positive (ER+) subsets. **B:** The frequency of *TOM1L1* amplification was assessed in the 61 *ERBB2*-amplified breast cancers of A that were classified according to their ER status. *TOM1L1* amplification was significantly more frequent in ER+ than in ER- *ERBB2* amplified tumours (Chi2 statistical test).

	TOM1L1 + N(%)	TOM1L1 - N (%)	<i>P</i>
ER +	17 (28%)	43 (72%)	0.027
ER -	4 (10%)	37 (90%)	
HER2 +	12 (44%)	15 (56%)	0.001
HER2 -	9 (12%)	65 (88%)	

Supplementary Table 3 (related to Fig. 1) The expression of TOM1L1 was assessed in 101 breast cancers and was classified according to their ER and HER2 clinical status. TOM1L1 expression was significantly more frequent in ER+ than in ER- tumours and in HER2+ than in HER2- tumours (Fisher's exact test).

Sequence	Modifications	Mass	Charges	PEP	Score	Ratio H/L	Ratio H/L normalized	Phosphorylation Localization probability
DPYATSVGHLEK	Unmodified	1428,7249	2,3	5.913E-12	173,72	0,98	1,00	
EATNTTSEPSAPSQDLLDLSPSPR	Unmodified	2512,1929	2,3	1.6259E-21	225,74	0,92	1,01	
EATNTTSEPSAPSQDLLDLSPSPR	Phospho (STY)	2592,1592	2	2.0455E-05	117,03	1,86	2,05	EATNTTSEPSAPSQDLLDL(0.784)PS(0.216)PR
EFVKENLVK	Unmodified	1104,6179	2	0.0076586	76,679	1,10	1,15	
EYVLDLVK	Unmodified	977,54335	2	8.0214E-05	116,37	1,00	1,02	
GVQFPPEAEAEAR	Unmodified	1587,7529	2,3	6.0188E-16	121,79	0,95	1,05	
KGVQFPPEAEAEAR	Unmodified	1715,8479	2,3	3.821E-09	153,94	0,95	1,02	
LHSELDLVK	Unmodified	1070,543	2	3.8465E-05	123,35	0,98	1,00	
LHSELDLVK	Oxidation (M)	1086,5379	2	0.013058	76,064	1,00	1,02	
NSTVTLVPEIQIK	Unmodified	1384,7562	2	9.6167E-09	156,24	0,98	1,00	
QETAQISSNPPTSVPAPALSSVIAPK	Unmodified	2690,4127	2,3	1.1835E-08	141,36	0,95	0,97	
SDLQPPNYYEVMFDFLAPAVTTEAIYEEIDAHQHK	Oxidation (M)	4175,931	4	0.0006373	83,633	0,95	0,97	
SDLQPPNYYEVMFDFLAPAVTTEAIYEEIDAHQHK	Unmodified	4159,9361	4	9.992E-06	103,68	0,94	0,96	
TWSQGFPGGVDVSEVK	Unmodified	1691,8155	2,3	3.9388E-29	244,05	0,92	0,94	
VMSAILMENTPGSENHEDIELLQK	Unmodified	2697,299	2,3,4	1.0051E-27	238,69	0,90	0,92	
VMSAILMENTPGSENHEDIELLQK	Oxidation (M)	2713,2939	2,3	4.5541E-09	158,92	0,92	0,93	
YNLPLDIQNR	Unmodified	1244,6513	2	1.5118E-11	180,07	0,97	1,07	

Supplementary Table 4 (related to Fig. 8) Mass-spectrometry: Identified human-TOM1L1 peptides after trypsin digestion. The table shows the peptide sequences, H/L SILAC ratio (light: Lapatinib; heavy: DMSO) and localization probability of phosphorylation sites (red).

TOM1L1-F	5'-GCTTCCCAGGAGGTGTGGAT-3'
TOM1L1-R	5'-TGAGGGAGGAAACTGAACGC-3'
ERBB2-F	5'-CCTATGCTGCCTCTTAGACCA-3'
ERBB2-R	5'-TTGCAATCTGCATACACCAG-3'
RPS6KB1-F	5'-ACTTCCAATACGACAGCCGAA-3'
RPS6KB1-R	5'-TTCATACGCAGGTGCTCTG-3'
PPM1D-F	5'-ATTGAAAGAACCCTCCAACAA-3'
PPM1D-R	5'-GCCATTTCTGTCTATGCTTCTTCAT-3'
CLTC-F	5'-CAATTTTGGACGTTTGGCATC-3'
CLTC-R	5'-AGCAGACCTCTTTCCATGTTCg-3'
DCK-F	5'-GCCGCCACAAGACTAAGAAT-3'
DCK-R	5'-CGATGTTCCCTTCGATGGAg-3'
ALB-F	5'-GCTGTCATCTCTTGTGGGCTgT-3'
ALB-R	5'-ACTCATGGGAGCTGCTGGTTC-3'
GAPDH-F	5'-GAAGGTGAAGGTCGGAGTC-3'
GAPDH-R	5'-GAAGATGGTGATGGGATTTC-3'
28S-F	5'-CGATCCATCATCCGCAATG-3'
28S-R	5'-AGCCAAGCTCAGCGCAAC-3'

Supplementary Table 5: Primers used for the RT-qPCR analysis (F: forward; R: reverse)